ECCM18 - 18^{th} European Conference on Composite Materials
Athens, Greece, 24^{th} – 28^{th} June 2018

Multiscale Virtual Testing Analysis for Thermoplastic Composites Using Response Surface Models for Design Optimization

Orestis Friderikos[1], Emmanuel Baranger[1], Damien Guillon[2]

1 : LMT, ENS-Cachan, CNRS, Université Paris-Saclay
61 avenue du Président Wilson, F- 94235 Cachan Cedex, France
e-mail : friderikos@lmt.ens-cachan.fr, emmanuel.baranger@ens-paris-saclay.fr
2 : Technocampus Composites Z.I. du Chaffault, 44340, Bouguenais, France
e-mail : Damien.Guillon@cetim.fr

Keywords : Virtual Testing Analysis, Global-local approach, Cohesive Zone Modeling, Least Squares, Multi-Stage Least Squares

Abstract
A mutliscale methodology has been introduced for determining the early stages of damage evolution in Quilted Stratum Process (QSP) [1] thermoplastic composite parts and answer critical design questions on why, where, and when damage and fracture initiates. A Virtual Testing Analysis (VTA) is developed using a global-local method based on the decomposition of a structure into a number of Representative Structural Components (RSC). The proposed software aims to augment FEA, with a hierarchical modeling that goes down to the meso-scale where a detailed modeling of each substructural component is performed using non-linear FEA. A key aspect of the VTA is that off-line computations for the RSC can be stored and used for different global scale structures as a simple failure criterion.

1. Introduction

Under the VTA framework a damage analysis to determine the early stages of degradation evolution under service loading is introduced. Physics based composite damage and failure mechanisms are used to interrogate the structural response. The evaluation of damage and failure criteria are implemented at the important structural details (local) and appropriate stiffness degradation functions with a pre-defined tolerance are reflected in the structural stiffness. As a benchmark test case, the simulation of interlaminar composite failures, namely delamination initiation/growth mechanisms of an internal ply drop-off laminate is considered using Cohesive Zone Modeling [2,3]. An essential part of the VTA concerns the generation of a high dimensional design space for each local substructure using variables corresponding to the operating loading conditions, material orientation angles and geometric features. Different Design of Computer Experiments (DCE) methods are implemented for sampling the design space as for example Latin Hypercube Sampling (LHS), sampling subjected to constraints, etc. Hence, a large-scale system identification problem arise in the estimation of the parameters of polynomial approximations.
A Linear Least Squares (LLS) method for constructing polynomial approximations as well as a novel Multi-Stage Least Squares (MSLS) approach is presented as an alternative approximation for the design and analysis of computer experiments. The MSLS relies on a variable separation into sets which yields locally optimal solutions in each subspace. The separation of variables produces a significant reduction in the dimensionality of the problem. In MSLS, LLS minimization problems are defined in each stage where different polynomial order approximations can also be applied. Preliminary results showed a higher accuracy of MSLS in comparison to LLS with a significant reduction in the computational complexity of more than two orders of magnitude. Error analysis of LLS and MSLS is performed along with a graphical comparison of the approximations.

2. General overview of the Multiscale global-local methodology

The multiscale methodology augments finite element software by providing progressive failure analysis based on damage tracking and material property degradation at the meso-scale, where damage and delamination have their source. The global/local overall process designed to couple two separate Abaqus/Standard analysis is illustrated in Fig. 1 and can be summarized in the following steps :

1) A global structural analysis is realized to evaluate the structural response subjected to the operating design loads. The global structures are modeled and analyzed using conventional shell elements to keep the modeling and computational effort affordable. During this step, the loading conditions at the boundaries of the important structural details are extracted using Abaqus Submodeling [4] in order to be transferred to the local scale as boundary conditions for non-linear FEM computations.
2) A decomposition of the composite part and detailed modeling of the structural components (e.g., stiffeners, tapering of the thickness of a laminate by terminate, or dropping, internal or external plies, corners) (see Fig. 1), henceforth called Representative Structural Component (RSC) problems is performed. These local problems are modeled using a nonlinear FE analysis (Abaqus/Standard). In the later, solid elements with cohesive elements or cohesive surfaces are introduced to evaluate the various delamination modes [2,3].
3) DCE methods are implemented for an efficient sampling of the design space using LHS, sampling subjected to constraints, etc.
4) A Response Surface (RS) method is used for constructing polynomial approximations using LLS or the novel MSLS approach which is proposed as an alternative approximation for the design and analysis of computer experiments. RS is applied to the data of the design space in order to define a set of criteria describing the various failure modes of the RSC. These criteria may involve not only the macroscopic loading but also the material properties of the plies related to different fiber orientations as well as the geometry of the laminate defined by the local stacking sequence. Thus, it is possible to study the design limits of the established criteria vis a vis reference configurations in order to define the application of the model range.
5) Determination of the RSC stiffness loss in reference directions based on a Linear Perturbation Analysis performed during the FEA.
6) Design of failure envelopes for a damaged state that corresponds to a predefined reduction of the RSC laminate stiffness in reference directions.

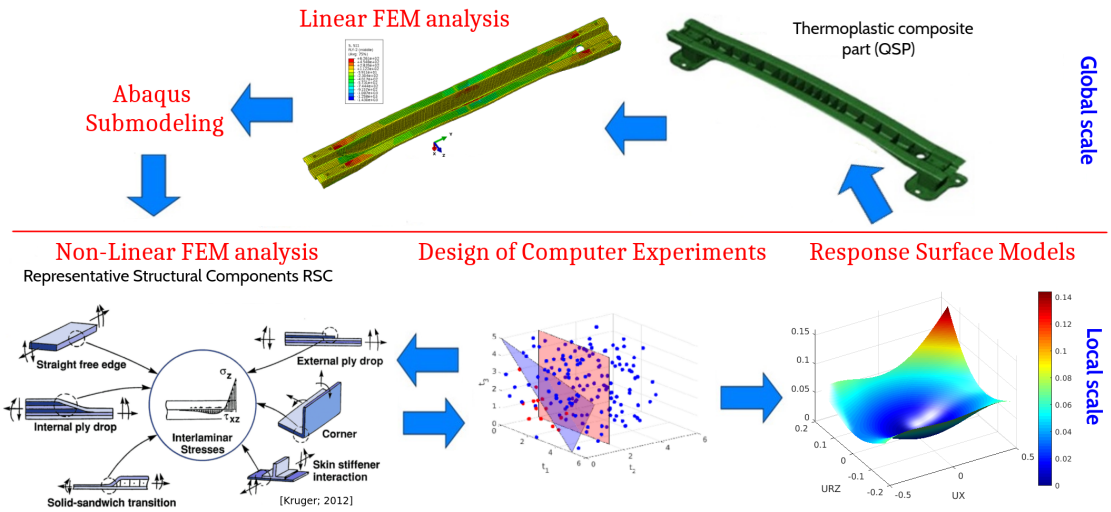

Fig. 1.*: Virtual Testing Analysis flowchart for QSP thermoplastic composite parts.*

3. Local scale - Cohesive Zone Modeling in Abaqus

3.1. Cohesive Zone Modeling (CZM)

The basic hypothesis of the CZM is that all the inelastic effects that occur at the vicinity of a crack can be lumped into a surface, the cohesive damage zone. Cohesive damage zone models relate tractions t to displacement jumps δ at an interface where a crack develops. Damage initiation is related to the nominal cohesive strength t° ; when the area under the traction-displacement jump relation is equal to the critical energy release rate, G^c, the traction is reduced to zero and new crack surfaces are formed. The new crack

surfaces are completely formed when the displacement jump is equal or greater that the displacement jump at complete failure δ^f. Using the definition of the J integral, it can be shown that for small cohesive zones [2]

$$\int_0^{\delta^f} t(\delta)d\delta = G^c \tag{Eq. 1}$$

A bi-linear triangular cohesive law for failure analysis is used for pure Mode I and pure Mode II or Mode III. The form of the cohesive law is dependent on the corresponding cohesive strength, interfacial stiffness (penalty stiffness, K) and the critical strain energy release rate.

$$t = \begin{cases} K\delta, & \delta \leq \delta^\circ \\ (1-d)K\delta, & \delta^\circ < \delta < \delta^f \\ 0, & \delta \geq \delta^f \end{cases} \tag{Eq. 2}$$

A mixed-mode criterion accounting for the effect of the interaction of the traction components in the onset of delaminaton is used. Damage initiation is predicted using a quadratic failure criterion considering nominal stresses where compressive normal tractions do not affect delamination onset :

$$\left\{\frac{\langle t_n \rangle}{t_n^\circ}\right\}^2 + \left\{\frac{t_s}{t_s^\circ}\right\}^2 + \left\{\frac{t_t}{t_t^\circ}\right\}^2 = 1 \tag{Eq. 3}$$

where t_s°, t_s° and t_t° are the nominal cohesive strengths in normal and the two shear directions, respectively and $\langle\rangle$ is the Macaulay bracket notation denoting the positive part.
In order to accurately account for the variation of fracture toughness as a function of mode ratio, a mixed-mode energy-based damage evolution criterion proposed in [5] is used

$$G^c = G_n^c + (G_s^c - G_n^c)\left(\frac{G_s}{G_n + G_s}\right)^n \tag{Eq. 4}$$

where n is the semi-empirical criterion exponent applied to delamination initiation and growth.

3.2. Simulation of the debonding mechanisms of internal ply drop-off laminates

Tapered laminated structures are formed by dropping off some of the plies at discrete positions over the laminate. The inherent weakness of this construction is the presence of material and geometric discontinuities at ply drop region that induce premature interlaminar failure at interfaces between dropped and continuous plies and may cause a significant loss of structural integrity. In the foregoing simulations of internal ply drop-off laminates, the geometry of the resin pocket is idealized to be right triangular shaped which represents a worst-case scenario, i.e., it is more prone to delamination than other triangular shapes (especially in the thin section) [6]. Hence, a minimization of the number of parameters needed to describe the ply-drop geometry is accomplished. Furthermore, the resin pocket is considered as a void in order to increase the stress intensity factors in the local models. This promotes thin section delamination, while the onset and growth of interlaminar cracks in the thick section are both unaffected by the material/geometrical properties of the resin pocket [7,8].
A benchmark ply drop-off model comprised of three composite 0° plies with uniform thickness of 1 mm subjected to static tensile loading using prescribed displacements of $u_x = 0.25$ mm is presented in Fig. 2. The scalar damage variable of the cohesive elements (SDEG) presents the failure state of the cohesive zones (red color identifies completely damaged elements). Delamination starts from the root of the ply drop (thin section) followed by delamination propagation at the two cohesive zones at the thick ply drop section. Displacement discontinuity in the longitudinal direction-1 indicates Mode II fracture in both cohesive zones (Fig. 2.b) whereas displacement discontinuity in the transverse direction-2 resulting to Mode I fracture occurs only in the ply drop thin section cohesive zone (Fig. 2.c).
Furthermore, in order to reduce the computational complexity, an equivalent 2D ply drop off model is implemented using Surface-based cohesive behavior [4] which provides a simplified way to model

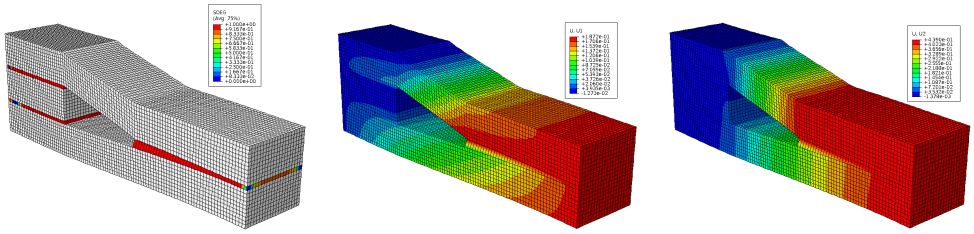

(a) *(b)* *(c)*

Fig. 2.: *Damage evolution of the benchmark ply drop model under static tensile loading; (a) SDEG of the cohesive elements; (b) Displacement discontinuity in longitudinal direction-1 (Mode II fracture); (c) Displacement discontinuity in the transverse direction-2 resulting to Mode I fracture only in the ply drop thin section cohesive zone.*

cohesive connections with negligible small interface thickness using the traction-separation constitutive law. Cohesive surface behavior is defined as a surface interaction property and a pure master-slave formulation is enforced for surfaces with cohesive behavior. It has to be mentioned that since it is not possible to take into account the different fiber orientations of the plies in the 2D case in Abaqus/Standard, a transformation of the material axes has been performed and a fully anisotropic tensor is defined using Matlab scripts for the 2D model.

3.3. Linear Perturbation Analysis (LPA) - Directional Stiffness Loss criterion

We aim to investigate the structure's integrity due to damage accumulation resulting from the delamination of the cohesive zone layers. A precise characterization of the structural response requires the knowledge of the structural stiffness loss in various reference directions when it is subjected to an arbitrary loading state. Consequently, a Linear Perturbation Analysis (LPA) is used and is postulated to be a measure of the structure's integridy. We perform LPA using a general analysis step to provide the linear response of the system. LPA is performed from time to time during the nonlinear analysis by including the linear perturbation steps between the general response steps. The linear perturbation response has no effect on the general analysis since the perturbation load is taken arbitrarily to be a very small number. LPA steps are performed in directions 1, 2 and rotation in direction 3 using prescribed displacements/rotations. Hence, LPA results to the evaluation of the Directional Stiffness Loss (DSL) functions $\mathrm{DSL}_{\mathrm{U1}}, \mathrm{DSL}_{\mathrm{U2}}$ and $\mathrm{DSL}_{\mathrm{UR3}}$ defined as $\mathrm{DSL} = (\mathbb{C}_0 - \mathbb{C})/\mathbb{C}_0$, where $\mathbb{C}_0$ and $\mathbb{C}$ are the initial and damaged stiffness at state n, respectively.

4. Design of Computer Experiments (DCE)

Latin hypercube sampling (LHS) is used for generating randomly distributed points in the design space corresponding to different ply material orientations [9]. LHS design created with the Matlab function lhsdesign with $d = 3$ dimensions and $SP = 40$ points. The design variables in this case corresponds to ply orientations angles $\theta_1^\circ, \theta_2^\circ, \theta_3^\circ$ of the three RSC plies, respectively. The design limits for the ply orientations are $0^\circ \leq \theta_1^\circ \leq 90^\circ, 0^\circ \leq \theta_2^\circ \leq 90^\circ, 0^\circ \leq \theta_3^\circ \leq 90^\circ$.
Sampling in the interior of the design space is not optimal when prescribed displacements/rotations are used since during FEM computations all the intermediate states are also evaluated. Hence, a design space sampling optimization can be obtained if the points are equally distributed on the surface of a n-dimensional sphere, i.e., if for example all prescribed displacements and rotations are considered, the sampling points must be uniformly distributed on the surface of a 6D sphere. In the 2D case, utilizing prescribed displacements UX and UY and rotation URZ, $N = 62$ sampling points are equi-distributed on the surface of a sphere with polar angle $\theta = \pi/6$ and azimuth angle $\phi = \pi/6$.
Opposed to the above cases, sampling of the design space for the ply drop off laminate thickness is not a trivial task since a number of geometrical constraints are required according to the final net shape design. These constraints concern the thickness of the individual plies of the laminate as well as the

overall structural thickness. Application of the LHS in a constraint space requires complex algorithms that cannot in general guarantee an optimal sampling, especially in high dimensional spaces. Henceforth, in the present analysis we introduced a non-optimal but simple procedure to sample the constraint design space. First, a LHS is performed using the minimum/maximum values of the design variables and at a following step the points that are not fulfill the geometrical constraints are rejected.

5. Procedure for Generating RSC Failure Envelopes

5.1. Linear Least Squares

The linear model is the main technique in regression problems and the primary tool for least squares fitting. LLS minimize a sum of squared errors, or equivalently the sample average of squared errors. That is a natural choice when one is interested in finding the regression function which minimizes the corresponding expected squared error. From the observed response values $y_1, y_2, ..., y_n$ and features x_{ij} for $i = 1, ..., n$ and $j = 1, ..., p$, LLS is obtain the parameter values $\alpha_1, ..., \alpha_p$ that minimize

$$\underset{\alpha_1,...,\alpha_p \in \mathbb{R}}{\arg\min}\ S(\alpha_1, ..., \alpha_p) = \sum_{i=1}^{n} \left(y_i - \sum_{j=1}^{p} x_{ij}\alpha_j \right)^2 \qquad \text{(Eq. 5)}$$

The minimizing values are denoted with hat symbols : $\hat{\alpha}_1, ..., \hat{\alpha}_p$. To minimize S, we set its partial derivative with respect to each α_j to 0. The solution satisfies

$$\frac{\partial}{\partial \alpha_j} S = -2 \sum_{i=1}^{n} \left(y_i - \sum_{j=1}^{p} x_{ij}\hat{\alpha}_j \right) x_{ij} = 0, \qquad j = 1, .., p \qquad \text{(Eq. 6)}$$

The p equations in (Eq. 6) are also known as the normal equations. Let us writing equations (Eq. 5) and (Eq. 6) in matrix notation where responses and feature values are represented via the vector $\mathbf{Y}$ and matrix $\mathbf{X}$. Let $\boldsymbol{\alpha} = (\alpha_1, ..., \alpha_p)^T$ and $\hat{\boldsymbol{\alpha}}$ denote the minimiser of the sum of squares. From the normal equations we find that

$$\hat{\boldsymbol{\alpha}} = (\mathbf{X}^T\mathbf{X})^{-1}\mathbf{X}^T\mathbf{Y} \qquad \text{(Eq. 7)}$$

where the matrix $\mathbf{X}^+ = (\mathbf{X}^T\mathbf{X})^{-1}\mathbf{X}^T$ is the Moore-Penrose inverse.

5.2. Multi-Stage Least Squares and Subspace Approximation

The Multi-Stage Least Squares algorithm (MSLS) can be viewed as a method which provides an optimal selection at each stage locally so as to obtain a globally optimum solution. Using a selection of subsets of the regression variables, the MSLS yield locally optimal solutions in each subspace where different polynomial order approximations can be applied. In summary, implementation of MSLS consists of minimizing the first subspace and then using the optimal values obtained for the estimated parameters as an input to solve the minimization problem in the second subspace. This procedure is followed sequentially for all subspaces and a global minimum is found at the end of the process. MSLS can be outlined in the subsequent steps.

5.2.1. Selection of Subsets of Regression Variables

Let at assume vectors $\mathbf{x^L}, \mathbf{x^\Theta}, \mathbf{x^G}$ corresponding to different sets of variables as follows

$$\mathbf{x} = \{\underbrace{x_1\ x_2\ \cdots\ x_{n1}}_{\mathbf{x^L}}\ \underbrace{x_{n1+1}\ x_{n1+2} \cdots x_{n1+n2}}_{\mathbf{x^\Theta}}\ \underbrace{x_{n2+1}\ x_{n2+1} \cdots x_{n2+n3}}_{\mathbf{x^P}}\}^T = \{\mathbf{x^L} \quad \mathbf{x^\Theta} \quad \mathbf{x^P}\}^T \qquad \text{(Eq. 8)}$$

where $\mathbf{x^L} \in \mathbb{R}^p$, $\mathbf{x^\Theta} \in \mathbb{R}^q$, $\mathbf{x^G} \in \mathbb{R}^r$, $p + q + r = n$ in a way that the following LS problems can be defined in different subspaces. In our case, $\mathbf{x^L}$ denote the loading variables, $\mathbf{x^\Theta}$ denote variables related to the material orientation angles and $\mathbf{x^G}$ denote variables related to geometry configurations.

5.2.2. First-Stage Least Squares

In the subspace spanned by the variables $\mathbf{x}^{\mathbf{L}}$ we need to solve $(k \times m)$ minimization problems for every fixed $\mathbf{x}^{\mathbf{\Theta}_i}, \mathbf{x}^{\mathbf{G}_j}$ in the design space $\mathcal{H}$ under consideration.

$$\underset{\alpha_1,...,\alpha_{p_1}\in\mathbb{R}}{\arg\min}\ S_1(\alpha_1, ..., \alpha_{p_1}) = \left\| \mathbf{g} - \mathbf{L}(\mathbf{x}^{\mathbf{L}})\boldsymbol{\alpha}(\mathbf{x}^{\mathbf{\Theta}_i}, \mathbf{x}^{\mathbf{G}_j}) \right\|_{L_2}^2 \tag{Eq. 9}$$

and estimate parameter vectors $\hat{\boldsymbol{\alpha}}(\mathbf{x}^{\mathbf{\Theta}_i}, \mathbf{x}^{\mathbf{G}_j})$, $i = 1, 2, \cdots, k$, $j = 1, 2, \cdots, m$.

5.2.3. Second-Stage Least Squares

In the subspace spanned by the variables $\mathbf{x}^{\mathbf{\Theta}}$ we need to solve $(P_1 \times m)$ minimization problems for every fixed $\mathbf{x}^{\mathbf{G}_j}$ in the design space $\mathcal{H}$ under consideration.

$$\underset{\beta_1,...,\beta_{P_2}\in\mathbb{R}}{\arg\min}\ S_2(\beta_1, ..., \beta_{p_2}) = \left\| \hat{\boldsymbol{\alpha}}_{n1}^{\mathbf{\Theta},\mathbf{G}_j} - \mathbf{\Theta}(\mathbf{x}^{\mathbf{\Theta}})\boldsymbol{\beta}_{n1}(\mathbf{x}^{\mathbf{G}_j}) \right\|_{L_2}^2 \tag{Eq. 10}$$

with $\hat{\boldsymbol{\alpha}}_{n1}^{\mathbf{\Theta},\mathbf{G}_j} = \{\hat{\alpha}_{n1}^{\mathbf{\Theta}_1,\mathbf{G}_j} \quad \hat{\alpha}_{n1}^{\mathbf{\Theta}_2,\mathbf{G}_j} \quad \cdots \quad \hat{\alpha}_{n1}^{\mathbf{\Theta}_k,\mathbf{G}_j}\}^T$, $n_1 = 1, 2, \cdots, P_1$, $j = 1, 2, \cdots, m$
and estimate parameter vectors $\hat{\boldsymbol{\beta}}_{n1}(\mathbf{x}^{\mathbf{G}_j})$.

5.2.4. Third-Stage Least Squares

In the subspace spanned by the variables $\mathbf{x}^{\mathbf{G}}$ we need to solve $(P_1 \times P_2)$ minimization problems

$$\underset{\gamma_1,...,\gamma_{P_3}\in\mathbb{R}}{\arg\min}\ S_3(\gamma_1, ..., \gamma_{p_3}) = \left\| \hat{\boldsymbol{\beta}}_{n1,n2}^{\mathbf{G}} - \mathbf{G}(\mathbf{x}^{\mathbf{G}})\boldsymbol{\gamma}_{n1,n2} \right\|_{L_2}^2 \tag{Eq. 11}$$

with $\hat{\boldsymbol{\beta}}_{n1,n2}^{\mathbf{G}} = \{\hat{\beta}_{n1,n2}^{\mathbf{G}_1} \quad \hat{\beta}_{n1,n2}^{\mathbf{G}_2} \quad \cdots \quad \hat{\beta}_{n1,n2}^{\mathbf{G}_m}\}^T$, $n_1 = 1, 2, \cdots, P_1$, $n_2 = 1, 2, \cdots, P_2$
and finally estimate parameter vectors $\hat{\boldsymbol{\gamma}}_{n1,n2}$.

5.2.5. Reconstruction of the analytical function

Finally, the reconstruction of the analytical function can be expressed as

$$\hat{g}(\mathbf{x}^{\mathbf{L}}, \mathbf{x}^{\mathbf{\Theta}}, \mathbf{x}^{\mathbf{G}}) = \sum_{i}^{P_1} \hat{\alpha}_i(\mathbf{x}^{\mathbf{\Theta}}, \mathbf{x}^{\mathbf{G}}) f_i(\mathbf{x}^{\mathbf{L}}) = \sum_{i}^{P_1} \left[\sum_{j}^{P_2} \hat{\beta}_j^i(\mathbf{x}^{\mathbf{G}}) h_j(\mathbf{x}^{\mathbf{\Theta}}) \right] f_i(\mathbf{x}^{\mathbf{L}}) =$$

$$\sum_{i}^{P_1} \left[\sum_{j}^{P_2} \left[\sum_{k}^{P_3} \hat{\gamma}_k^{i,j} q_k(\mathbf{x}^{\mathbf{G}}) \right] h_j(\mathbf{x}^{\mathbf{\Theta}}) \right] f_i(\mathbf{x}^{\mathbf{L}}) \tag{Eq. 12}$$

where $\hat{\beta}_j^i$: j parameter estimation of $\hat{\alpha}_i$ and $\hat{\gamma}_k^{i,j}$ is the k parameter estimation of $\hat{\beta}_j^i$, $i = 1, ..., P_1$, $j = 1, ..., P_2$, $k = 1, ..., P_3$.

6. Numerical Tests

Numerical tests have been performed to evaluate the approximation of the LLS and MSLS method. Furthermore, in order to gain further insight into the non-linear structure of the DSL manifold in a lower dimensional space, we consider a 3D space where an analytical function of the DSL is estimated by fixing one of the loading variables, i.e., x_2 = const, and therefore considering only two loading variables $\mathbf{x}^{\mathbf{L}} = \{x_1, x_3\}$, and generating failure graphs for the three variables corresponding to the material orientation angles sampling points $\mathbf{\Theta}_i(\mathbf{x}^{\mathbf{\Theta}})$; $\mathbf{x}^{\mathbf{\Theta}} = \{x_4, x_5, x_6\}$ and the three variables related to the ply laminate thickness sampling points $\mathbf{G}_j(\mathbf{x}^{\mathbf{G}})$; $\mathbf{x}^{\mathbf{G}} = \{x_7, x_8, x_9\}$ of the RSC part.

6.1. Linear Least Squares

For the approximation of the DSL manifold, a quadratic ($d = 2, n = 9$) and a 4-order polynomial equation ($d = 4, n = 9$) are used, resulting to the estimation of $\binom{n+d}{n}$=55 and 715 parameters, respectively. The coefficient of determination R^2 and the RMS value are computed for both equations in order to evaluate the gain of the LLS approximation using different polynomial order. Due to the large number of combinations between the variables of the 9D design space, we will provide some illustrative examples of the LLS approximation in a 3-D space. Figure 3 shows a surface plot of the LLS approximation using a 4-order polynomial for the DSL_{U1} (LPA in U1 direction) corresponding to the material orientation sampling point $\mathbf{\Theta}_1(\theta_1 = 40.48°, \theta_2 = 53.26°, \theta_3 = 25.70°)$ for two goemetric sampling points $\mathbf{G_1}(t_1 = 0.85, t_2 = 1.30, t_3 = 1.39)$ and $\mathbf{G_3}(t_1 = 1.61, t_2 = 1.17, t_3 = 1.19)$, respectively. Fig. 4 illustrates the coefficient of determination R^2 and the RMS of the quadratic and 4-order model for each configuration $\mathbf{\Theta}_i = \mathbf{\Theta}_i(\theta_1, \theta_2, \theta_3)$, $i = 1, 2, ...k$, where k is the number of different composite layups related to the sampling point $\mathbf{G_1}(t_1 = 0.85, t_2 = 1.30, t_3 = 1.39)$. As evidenced by the high R^2 values close to unity, the 4-order model appears to capture a large portion of the observed variance and is more accurate than the quadratic model.

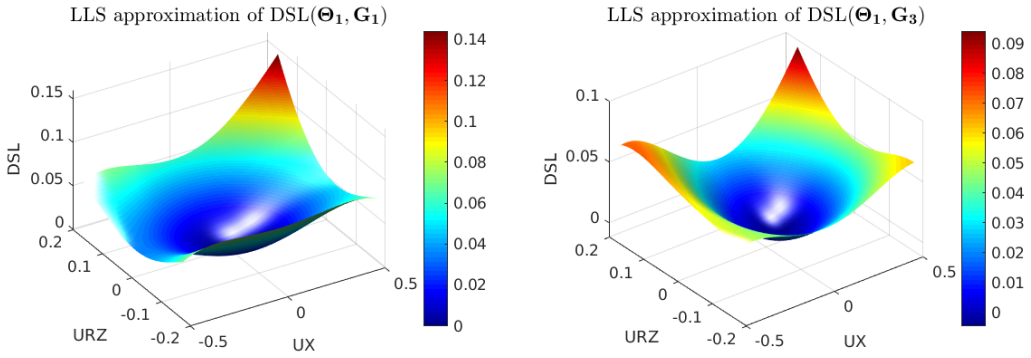

(a) *(b)*

Fig. 3.*: LLS approximation using a 4-order polynomial; a) $DSL_{UI}(\mathbf{\Theta_1}, \mathbf{G_1})$, b) $DSL_{UI}(\mathbf{\Theta_1}, \mathbf{G_3})$; $\mathbf{\Theta}_1(\theta_1 = 40.48°, \theta_2 = 53.26°, \theta_3 = 25.70°)$, $\mathbf{G_1}(t_1 = 0.85, t_2 = 1.30, t_3 = 1.39)$, $\mathbf{G_3}(t_1 = 1.61, t_2 = 1.17, t_3 = 1.19)$.

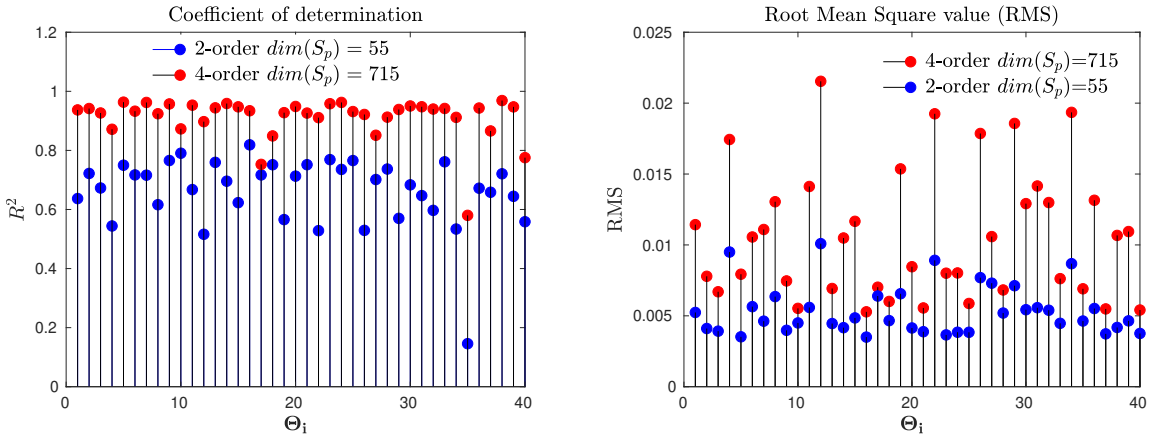

(a) *(b)*

Fig. 4.*: Coefficient of determination R^2 and RMS corresponding to a quadratic and a 4-order polynomial equation model for each configuration $\mathbf{\Theta}_i = \mathbf{\Theta}_i(\theta_1, \theta_2, \theta_3)$, $i = 1, 2, ...k$, where k is the number of different composite layups related to the sampling point $\mathbf{G_1}(t_1 = 0.85, t_2 = 1.30, t_3 = 1.39)$.*

6.2. Multi-Stage LS

At the First-Stage approximation, a 4-order polynomial equation ($d = 4, n = 3$) is used, resulting to the estimation of $\binom{n+d}{n}$=35 parameters, whereas at the Second and the Third-Stage, a cubic ($d = 3, n = 3$) and a quadratic ($d = 2, n = 3$) polynomial equation is used resulting to the estimation of 20 and 10 parameters, respectively. Figure 5 shows a surface plot of the MSLS approximation for the First and the Second- Stage MSLS of the DSL_{U1} corresponding to the material orientation sampling point $\mathbf{\Theta}_1(\theta_1 = 40.48°, \theta_2 = 53.26°, \theta_3 = 25.70°)$ and goemetric sampling point $\mathbf{G_1}(t_1 = 0.85, t_2 = 1.30, t_3 = 1.39)$. Furthermore, it is worth to underline that in the present application, MSLS provides a reduction in the computational complexity over two orders of magnitude as compared to LLS with almost the same level of accuracy (Figure 6).

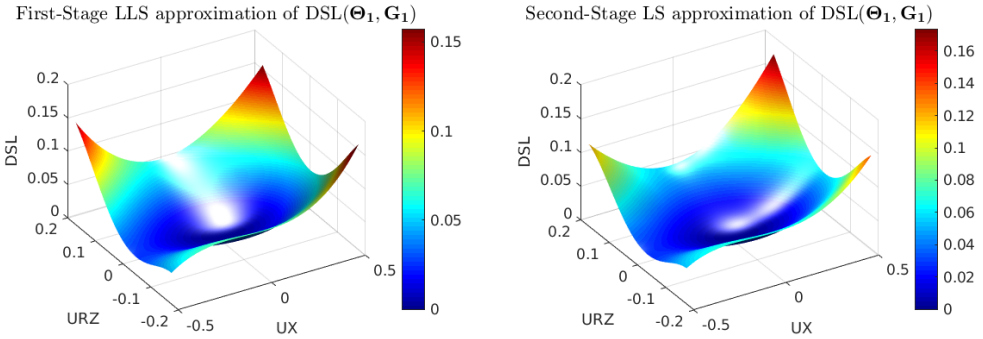

Fig. 5.*: MSLS approximation of $DSL_{U1}(\mathbf{\Theta_1}, \mathbf{G_1})$; a) First-Stage MSLS approximation ($d = 4, n = 3$), b) Second-Stage MSLS approximation ($d = 3, n = 3$).*

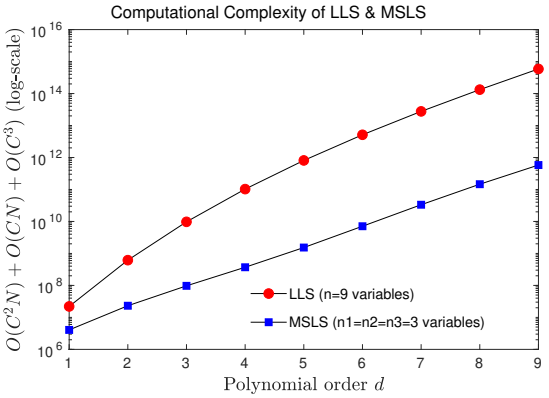

Fig. 6.*: Computational complexity of the LS and the Multi-Stage LS.*

7. Conclusions

The overall goal of this effort is to perform certification-by-analysis, utilizing an accurate VTA approach in combination with a reduced physical test data to decrease the design cycle time and cost for QSP thermoplastic composite parts. To this end, failure criteria based on a tolerance of stiffness loss for the composite part in order to achieve a robust design are determined.

References

[1] D. Guillon, A. Lemasçon and C. Callens. QSP : An innovative process based on tailored preforms for low cost and fast production of optimized thermoplastic composite parts. *ECCM17-17th European Conference on Composite Materials*, Germany, 2016.

[2] P.P. Camanho, C.G. Davila and D.R. Ambur. Numerical Simulation of Delamination Growth in Composite Materials. *NASATP-2001-211041*, 2001.
[3] R. Krueger. Development of benchmark examples for quasi-static delamination propagation and fatigue growth predictions. *SIMULIA Community Conference*, Providence, RI, May 14-17, 2012.
[4] ABAQUS 6.14 User's Manual, ABAQUS. Dassault Systèmes Simulia Corp., Providence, RI, USA.
[5] M.L. Benzeggagh and M. Kenane. Measurement of mixed-mode delamination fracture toughness of unidirectional glass/epoxy composites with mixed-mode bending apparatus. *Composites Science and Technology*, 56 :439-449, 1996.
[6] G. Allegri, M.R. Wisnom and S.R. Hallett. A simplified approach to the damage tolerance design of asymmetric tapered laminates. Part II : methodology validation. *Composites Part A*, 41(10), 1395–1402, 2010.
[7] W. Cui, M.R. Wisnom and M.I. Jones. An experimental and analytical study of delamination of unidirectional specimens with cut central plies. *Journal of Reinforced Plastics and Composites*, 13, 722–739, 1994.
[8] Z. Petrossian and M.R. Wisnom. Parametric study of delamination in composites with discontinuous plies using an analytical solution based on fracture mechanics. *Composites Part A*, 29A, 403–414, 1998.
[10] J.R. Koehler and A.B. Owen. Computer Experiments. *Handbook of Statistics (Ghosh, S. and Rao, C. R., eds.)*. Elsevier Science, New York, 261-308, 1996.